

CONF-761059-2

Submitted to

Proceedings of Small Accelerator Conference

Denton, TX

Oct. 25-27, 1976

Dr. John H. Thorngate

By acceptance of this article, the publisher or
recipient acknowledges the U. S. Government's right
to retain a non-exclusive, royalty-free license in
and to any copyright covering the article.

MEASUREMENTS OF DISTRIBUTIONS OF ENERGY LOSS AND ADDITIVITY OF ENERGY LOSS
FOR 50 TO 150 keV PROTONS IN HYDROGEN AND NINE HYDROGEN GASES*

John H. Thorngate

Health Physics Division
Oak Ridge National Laboratory
Oak Ridge, Tennessee 37830

Summary

Detailed measurements of energy-loss distributions were made for 51, 102 and 153 keV protons traversing hydrogen, methane, ethyne, ethene, ethane, propyne, propadiene, propene, cyclopropane and propane. Less detailed measurements were made at 76.5 and 127.5 keV. To simplify comparison with theory, all of the measurements were made at a gas density that gave a 4% energy loss. The mean energy, second central moment (a measure of the width of the distribution) and the third central moment (a measure of the skew) were calculated from the measured distributions. Stopping power values, calculated using the mean energy, agreed with the predictions of the theory by Bethe. For the second and third central moments, the best agreement between measurement and theory was obtained when the classical scattering probability was used for the calculations; but the agreement was not good. In all cases, variations were found in the data that could be correlated to the type of carbon binding in the molecule.

Introduction

The energy lost by charged particles as they traverse matter was first studied in the antiquity of the nuclear age. Within a few years of the discovery of natural radioactivity by Becquerel (1896), Bragg had made alpha-range measurements and Rutherford had made energy-loss measurements.

By 1913, Bohr¹ had published a theoretical explanation of the energy loss of charged particles passing through matter. Two other important phenomena were also studied quite early. In 1905,

Bragg and Kleeman² noted that the stopping power of a molecule was apparently the sum of the stopping powers of its constituent atoms, and by 1910

Geiger³ had made quantitative measurements of the increase in the width of the energy distribution of alpha particles that had traversed a stopping medium, an effect noted by Rutherford in his early work.

This paper describes measurements of proton energy-loss distributions in hydrocarbon gases at energies below 200 keV. Although Park and

Schowengerdt⁴ described an excellent facility for such measurements in 1969, their subsequent work has been devoted to cross section measurements rather than the type of energy-loss measurements described in this paper. Several workers have

MASTER

—NOTICE—
This report was prepared as an account of work sponsored by the United States Government. Neither the United States nor the United States Energy Research and Development Administration, nor any of their employees, nor any of their contractors, subcontractors, or their employees makes any warranty, express or implied, or assumes any legal liability or responsibility for the accuracy, completeness or usefulness of any information, apparatus, product or process disclosed, or represents that its use would not infringe privately owned rights.

butions were made for 51, 102 and 153 keV protons traversing hydrogen, methane, ethyne, ethene, ethane, propyne, propadiene, propene, cyclopropane and propane. Less detailed measurements were made at 76.5 and 127.5 keV. To simplify comparison with theory, all of the measurements were made at a gas density that gave a 4% energy loss. The mean energy, second central moment (a measure of the width of the distribution) and the third central moment (a measure of the skew) were calculated from the measured distributions. Stopping power values, calculated using the mean energy, agreed with the predictions of the theory by Bethe. For the second and third central moments, the best agreement between measurement and theory was obtained when the classical scattering probability was used for the calculations; but the agreement was not good. In all cases, variations were found in the data that could be correlated to the type of carbon binding in the molecule.

Introduction

The energy lost by charged particles as they traverse matter was first studied in the antiquity of the nuclear age. Within a few years of the discovery of natural radioactivity by Becquerel (1896), Bragg had made alpha-range measurements and Rutherford had made energy-loss measurements.

By 1913, Bohr¹ had published a theoretical explanation of the energy loss of charged particles passing through matter. Two other important phenomena were also studied quite early. In 1905, Bragg and Kleeman² noted that the stopping power of a molecule was apparently the sum of the stopping powers of its constituent atoms, and by 1910

Geiger³ had made quantitative measurements of the increase in the width of the energy distribution of alpha particles that had traversed a stopping medium, an effect noted by Rutherford in his early work.

This paper describes measurements of proton energy-loss distributions in hydrocarbon gases at energies below 200 keV. Although Park and

Schowengerdt⁴ described an excellent facility for such measurements in 1969, their subsequent work has been devoted to cross section measurements rather than the type of energy-loss measurements described in this paper. Several workers have measured proton stopping cross sections in this energy region.^{5,6,7} One aspect of these data is that chemical bonding seems to affect stopping cross sections in molecules when the incident protons have energies below 150 keV. Comparable studies of Bragg-Kleeman additivity for alpha

MASTER

NOTICE
This report was prepared as an account of work sponsored by the United States Government. Neither the United States nor the United States Energy Research and Development Administration, nor any of their employees, nor any of their contractors, subcontractors, or their employees, makes any warranty, express or implied, or assumes any legal liability or responsibility for the accuracy, completeness or usefulness of the information, apparatus, product or process disclosed, or represents that its use would not infringe privately owned rights.

2

*Research sponsored by the Energy Research and Development Administration under contract with Union Carbide Corporation.

MEAN ENERGY LOSS AND ADDITIVITY OF ENERGY LOSSES
HYDROGEN AND NINE HYDROGEN GASES*

H. Thorngate

Physics Division
National Laboratory
Tennessee 37830

particle stopping cross sections have been made by Bourland and Powers⁸ and more recently by Lodhi and Powers.⁹ The present experiment was designed to repeat some of the existing proton measurements, to extend them to other gases and to measure energy-loss distributions rather than just mean energy losses. Detailed energy-loss distributions were made at 50, 100 and 150 keV and less detailed measurements were made at 75 and 135 keV. The gases studied were hydrogen, ethyne (acetylene), ethene (ethylene), ethane, propyne (methyl acetylene) propadiene (allene), propene (propylene), cyclopropane and propane.

Theory

As previously mentioned, Bohr¹ had published "On the Theory of the Decrease of Velocity of Moving Electrified Particles on Passing Through Matter" in 1913. His results were largely corroborated by the quantum mechanical derivation published in 1930 by Bethe.¹⁰ If the incident particle is non-relativistic and if shell effects are neglected, the theoretical expression for the energy lost per unit path length is

$$-\frac{dE}{dx} = \frac{4\pi z^2 e^4 ZN}{mv^2} \ln \left(\frac{2mv^2}{I} \right)$$

where z is the charge and v is the velocity of the incident particle, Z is the atomic number and N is the atomic density of the stopping medium and m is the mass of the electron. The parameter I is the mean excitation energy of the stopping medium and is defined by

$$\ln I = \sum_n f_n \ln(E_n - E_0)$$

where $E_n - E_0$ is the energy for excitation of the stopping medium from the state n and the f_n are the associated dipole oscillator strengths. Values for I are usually determined from experimental data.¹¹ A useful discussion of the theories involved in the calculation of the stopping power of heavy charged particles in matter has been published by Turner.¹²

Considerable effort has been expended to develop a theoretical description of the distributions of the energy losses that a heavy particle undergoes as it slows down. The problem is often defined by how much of the initial energy is lost as the particle traverses

Powers.⁹ The present experiment was designed to repeat some of the existing proton measurements, to extend them to other gases and to measure energy-loss distributions rather than just mean energy losses. Detailed energy-loss distributions were made at 50, 100 and 150 keV and less detailed measurements were made at 75 and 135 keV. The gases studied were hydrogen, ethyne (acetylene), ethene (ethylene), ethane, propyne (methyl acetylene) propadiene (allene), propene (propylene), cyclopropane and propane.

Theory

As previously mentioned, Bohr¹ had published "On the Theory of the Decrease of Velocity of Moving Electrified Particles on Passing Through Matter" in 1913. His results were largely corroborated by the quantum mechanical derivation published in 1930 by

Bethe.¹⁰ If the incident particle is non-relativistic and if shell effects are neglected, the theoretical expression for the energy lost per unit path length is

$$- \frac{dE}{dx} = \frac{4\pi z^2 e^4 ZN}{mv^2} \ln \left(\frac{2mv^2}{I} \right)$$

where z is the charge and v is the velocity of the incident particle, Z is the atomic number and N is the atomic density of the stopping medium and m is the mass of the electron. The parameter I is the mean excitation energy of the stopping medium and is defined by

$$\ln I = \sum_n f_n \ln(E_n - E_0)$$

where $E_n - E_0$ is the energy for excitation of the stopping medium from the state n and the f_n are the associated dipole oscillator strengths. Values for I are usually determined from experimental data.¹¹ A useful discussion of the theories involved in the calculation of the stopping power of heavy charged particles in matter has been published by Turner.¹²

Considerable effort has been expended to develop a theoretical description of the distributions of the energy losses that a heavy particle undergoes as it slows down. The problem is often defined by how much of the initial energy is lost as the particle traverses the medium. If the absorber is so thin that the energy of the particle can be considered unchanged, the process is well described, for particles above 10 MeV, by theories developed by Landau¹³ and Vavilov.¹⁴ For large energy losses, the first theory was published by Bohr¹⁵ in 1915 with more recent contributions by Tschalär¹⁶ and Payne.¹⁷

A useful theory for the intermediate energy-loss region, applicable to results from this experiment, was developed by Symon.^{18,19} Payne¹⁷ summarizes this theory in his work on thick absorbers and the following presentation will be based on this exposition.

The energy-loss distribution is generally denoted as $F(E, S)$, where $F(E, S)dE$ is the fraction of particles with energies between E and $E+dE$ after a path length, S , has been traversed in the stopping medium. Symon describes $F(E, S)$ in terms of its central moments,

$$\Lambda_n(S) = \int_0^\infty (E - \langle E \rangle)^n F(E, S) dE$$

where $\langle E \rangle = \int_0^\infty E F(E, S) dE$. These moments may be calculated easily from both theory and experiment. According to Payne, several Λ_n are required to describe the distribution for very thin or very thick absorbers, but $\langle E \rangle$, Λ_2 and Λ_3 should suffice when the energy losses are on the order of 3% of the initial energy, E_0 . This experiment was designed so that all of the measurements involved a 4% energy loss.

Subsequent moments may be related by differentiating the defining equation, which results in

$$\frac{d\Lambda_n(S)}{dS} = -n \frac{d\langle E \rangle}{dS} \Lambda_{n-1}(S) + \int_0^\infty (E - \langle E \rangle)^{n-1} \frac{\partial F(E, S)}{\partial S} dE.$$

Symon found this could be written as

$$\frac{d\Lambda_n(S)}{dS} = -n \frac{d\langle E \rangle}{dS} \Lambda_{n-1}(S) + \sum_{L=1}^n \frac{n!(-1)^L}{(n-L)!} \int_0^\infty M_L(E) (E - \langle E \rangle)^{n-L} F(E, S) dE ,$$

where

$$M_L = \frac{1}{L!} \int_0^\infty P(E, t) t^L dt .$$

Thus, if the proper probability function, $P(E, t)$, can be found, the $\Lambda_n(S)$ can be calculated.

$\Lambda_0(S)$ and $\Lambda_1(S)$ can be calculated directly from the defining equation. For $\Lambda_0(S)$ the results are

$$\Lambda_0(S) = \int_0^\infty F(E, S) dE .$$

This can be set equal to unity as a normalization requirement. When this is done $\Lambda_1(S) = 0$.

In his work, Bohr assumed that the distribution was a Gaussian, sharply peaked at $\langle E \rangle$, which is equivalent to assuming that the average rate of energy loss is the same for all protons. This is

$$A_n(S) = \int_0^\infty (E - \langle E \rangle)^n F(E, S) dE$$

where $\langle E \rangle = \int_0^\infty EF(E, S) dE$. These moments may be calculated easily from both theory and experiment. According to Payne, several A_n are required to describe the distribution for very thin or very thick absorbers, but A_2 and A_3 should suffice when the energy losses are on the order of 3% of the initial energy, E_0 . This experiment was designed so that all of the measurements involved a 4% energy loss.

Subsequent moments may be related by differentiating the defining equation, which results in

$$\frac{dA_n(S)}{ds} = -n \frac{d\langle E \rangle}{ds} A_{n-1}(S) + \int_0^\infty (E - \langle E \rangle)^{n-1} \frac{\partial F(E, S)}{\partial S} dE.$$

Symon found this could be written as

$$\frac{dA_n(S)}{ds} = -n \frac{d\langle E \rangle}{ds} A_{n-1}(S) + \sum_{L=1}^n \frac{n!(-1)^L}{(n-L)!} \int_0^\infty M_L(E) (E - \langle E \rangle)^{n-L} F(E, S) dE,$$

where

$$M_L = \frac{1}{L!} \int_0^\infty P(E, t) t^L dt.$$

Thus, if the proper probability function, $P(E, t)$, can be found, the $A_n(S)$ can be calculated.

$A_0(S)$ and $A_1(S)$ can be calculated directly from the defining equation. For $A_0(S)$ the results are

$$A_0(S) = \int_0^\infty F(E, S) dE.$$

This can be set equal to unity as a normalization requirement. When this is done $A_1(S) = 0$.

In his work, Bohr assumed that the distribution was a Gaussian, sharply peaked at $\langle E \rangle$, which is equivalent to assuming that the average rate of energy loss is the same for all protons. This implies that the $M_L(E)$ are constants. Symon improved this approximation by using the first two terms of an expansion of the $M_L(E)$ around $\langle E \rangle$, i.e.,

$$M_L(E) \approx M_L(\langle E \rangle) + (E - \langle E \rangle) \frac{dM_L(\langle E \rangle)}{d\langle E \rangle}.$$

2

As Payne points out, this allows a change in the width of the $F(E, S)$ with energy due to the fact that particles of different energies lose energy at different average rates. It also allows deviations from a Gaussian form. $M_L(\langle E \rangle) = 1$ and $\frac{dM_L(\langle E \rangle)}{d\langle E \rangle} = 0$.

$$\frac{d \langle E \rangle}{dS} = - \int_0^\infty M_{1\omega}(E) F(E, S) dE .$$

For this experiment, only $\langle E \rangle$, A_2 and A_3 need to be calculated. Using the approximate value of $M_1(E)$ gives

$$\frac{d \langle E \rangle}{dS} = - M_{1\omega}(\langle E \rangle) ,$$

$$\frac{dA_2(S)}{dS} = 2M_2(\langle E \rangle) - 2 \frac{dM_{1\omega}(\langle E \rangle)}{d \langle E \rangle} A_2(S) , \text{ and}$$

$$\frac{dA_3(S)}{dS} = -3 \frac{dM_{1\omega}(\langle E \rangle)}{d \langle E \rangle} A_3 + 6 \frac{dM_{2\omega}(\langle E \rangle)}{d \langle E \rangle} A_2 - 6M_3(\langle E \rangle) .$$

To evaluate these equations requires values for M_1 , M_2 and M_3 which in turn requires the selection of a $P(E, t)$. A convenient form is the classical scattering probability, given by Payne as

$$P(E, t) = K/Et^2 \quad \text{if } \frac{4mE}{M} \leq t \leq \frac{I^2 M}{4mE} \\ = 0 \quad \text{otherwise.}$$

The constant $K = \pi e^4 MNZ/m$ for protons where M is the mass of the proton and the other terms have the same meaning as in the stopping power theory. Using this probability function gives the Bethe formula for $d\langle E \rangle/dS$ which in turn can be used to integrate equations for A_2 and A_3 .

Additivity of stopping powers can be expressed in several ways with the choice for a particular application depending on what form the data are in and the end use of the results. It proved most useful to use stopping cross sections in this experiment. Stopping cross sections are expressed in units of

$\text{eV-cm}^2\text{-molecule}^{-1} \times 10^{-15}$ and are related to dE/dx by

$$\epsilon = \frac{1}{N} \frac{dE}{dx} .$$

Additivity is applied by calculating the stopping cross section for the compound $A_m B_n$ from the equation

$$\epsilon(A_m B_n) = m\epsilon(A) + n\epsilon(B) .$$

Apparatus and Procedures

A proton energy-loss experiment is conceptually simple, requiring three pieces of equipment: a source of protons, a chamber to hold the material under study, and a proton spectrometer. To measure energy losses of monoenergetic protons in gases adds several complications. First, simple accelerators, such as that available for this experiment, do not produce a monoenergetic proton beam. Second, some means must be devised to get the protons into and out of the cell holding the gas. In this experiment, an electrostatic analyzer was used to select a narrow interval

$$\frac{3}{dS} = -3 \frac{1}{d\langle E \rangle} A_3 + 6 \frac{1}{d\langle E \rangle} A_2 - 6M_3 \langle E \rangle.$$

To evaluate these equations requires values for M_1 , M_2 and M_3 which in turn requires the selection of a $P(E, t)$. A convenient form is the classical scattering probability, given by Payne as

$$P(E, t) = K/Et^2 \quad \text{if } \frac{4mE}{M} \leq t \leq \frac{I^2 M}{4mE}$$

$$= 0 \quad \text{otherwise.}$$

The constant $K = \pi e^4 MNZ/m$ for protons where N is the mass of the proton and the other terms have the same meaning as in the stopping power theory. Using this probability function gives the Bethe formula for $d\langle E \rangle/dS$ which in turn can be used to integrate equations for A_2 and A_3 .

Additivity of stopping powers can be expressed in several ways with the choice for a particular application depending on what form the data are in and the end use of the results. It proved most useful to use stopping cross sections in this experiment. Stopping cross sections are expressed in units of

$\text{eV-cm}^2\text{-molecule}^{-1} \times 10^{-15}$ and are related to dE/dx by

$$\epsilon = \frac{1}{N} \frac{dE}{dx} .$$

Additivity is applied by calculating the stopping cross section for the compound $A_m B_n$ from the equation

$$\epsilon(A_m B_n) = m\epsilon(A) + n\epsilon(B) .$$

Apparatus and Procedures

A proton energy-loss experiment is conceptually simple, requiring three pieces of equipment: a source of protons, a chamber to hold the material under study, and a proton spectrometer. To measure energy losses of monoenergetic protons in gases adds several complications. First, simple accelerators, such as that available for this experiment, do not produce a monoenergetic proton beam. Second, some means must be devised to get the protons into and out of the cell holding the gas. In this experiment, an electrostatic analyzer was used to select a narrow interval in the energy distribution of the protons produced by the accelerator (input analyzer). A differentially pumped gas cell held the gas under study and a second electrostatic analyzer was used to measure the spectrum of the protons emerging from the cell (output analyzer). A simplified diagram of the system is given in Figure 1.

2

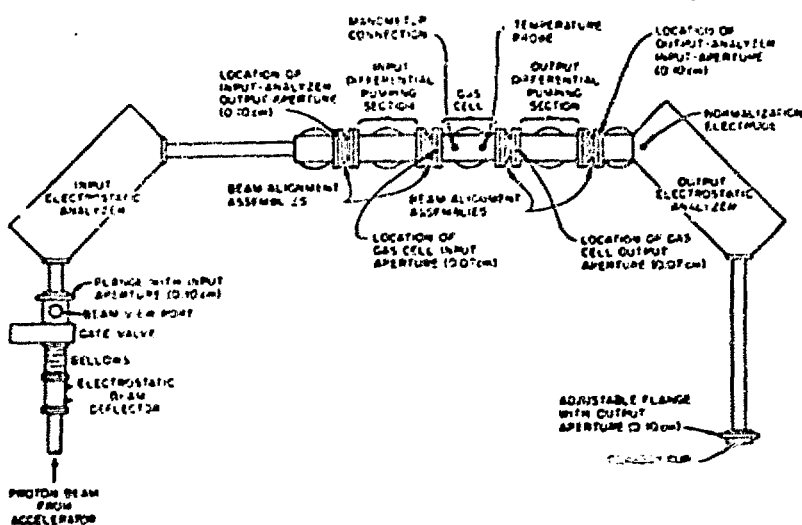


Fig. 1. Plan Diagram of the Experimental Equipment.

A Texas Nuclear Model 9999 accelerator was the source of the protons. This accelerator was designed as a neutron generator but, because it had a relatively sophisticated accelerating column with reasonably good ion optics, it was obtained with a mechanical gas valve and an R.F. ion source so that a wide range of ions might be accelerated. None of the voltage supplies on the machine were regulated or highly filtered, since such refinements are not necessary to produce neutrons. As a result, the beam energy fluctuated several keV.

The machine was designed to operate at 200 keV but it was not stable enough for use above 150 keV in this experiment. Maximum beams produced by the machine ranged from about 200 μ A at 50 keV to 400 μ A at 150 keV. Most of this current was lost in the collimation and energy selection required.

Unless a high-resolution spectrometer is used to measure the proton spectrum, some technique is required to unfold the contribution of the spectrometer from the data. Conversely, the detector response may be folded into the theoretical distribution for comparisons, but this approach has less value when the theory is not well developed. The analyzer pole pieces were 90° sectors of concentric spheres. Spherical pole pieces gave the analyzer twice the dispersion that could be obtained from an analyzer with cylindrical pole pieces and focussed the beam from a circular aperture into a spot rather than a line.

Design of the analyzers was based upon equations given by Siegbahn²⁰ and resulted in an instrument with a theoretical dispersion of just over 1000. The pole pieces had an inner radius of 14.75 inches (37.5 cm) and an outer radius of 15 inches (38.1 cm) which resulted in a gap of 0.25 inches (6.4 mm). Since the distance between the

Fig. 1. Plan Diagram of the Experimental Equipment.

A Texas Nuclear Model 9999 accelerator was the source of the protons. This accelerator was designed as a neutron generator but, because it had a relatively sophisticated accelerating column with reasonably good ion optics, it was obtained with a mechanical gas valve and an R.F. ion source so that a wide range of ions might be accelerated. None of the voltage supplies on the machine were regulated or highly filtered, since such refinements are not necessary to produce neutrons. As a result, the beam energy fluctuated several keV.

The machine was designed to operate at 200 keV but it was not stable enough for use above 150 keV in this experiment. Maximum beams produced by the machine ranged from about 200 μ A at 50 keV to 400 μ A at 150 keV. Most of this current was lost in the collimation and energy selection required.

Unless a high-resolution spectrometer is used to measure the proton spectrum, some technique is required to unfold the contribution of the spectrometer from the data. Conversely, the detector response may be folded into the theoretical distribution for comparisons, but this approach has less value when the theory is not well developed. The analyzer pole pieces were 90° sectors of concentric spheres. Spherical pole pieces gave the analyzer twice the dispersion that could be obtained from an analyzer with cylindrical pole pieces and focussed the beam from a circular aperture into a spot rather than a line.

Design of the analyzers was based upon equations given by Siegbahn²⁰ and resulted in an instrument with a theoretical dispersion of just over 1000. The pole pieces had an inner radius of 14.75 inches (37.5 cm) and an outer radius of 15 inches (38.1 cm) which resulted in a gap of 0.25 inches (6.4 mm). Size was dictated by the amount of space available for the experiment in the accelerator building and the requirement that the analyzer be capable of transmitting 500 keV protons with plus and minus 10 kV (or less) potentials applied to the electrodes. This decreased the problems that arise when insulators, cables and connectors must handle higher voltages.

The size of the input and exit apertures, coupled with the inherent dispersion of the analyzer, set the energy resolution at 0.1% (50 eV at 50 keV and 150 eV at 150 keV). A one volt change on either electrode corresponded to a 29 eV change in the energy of the charged particles transmitted by the analyzer. To be consistent with the resolution of the analyzer, the electrode potential of the output analyzer was changed in 2 volt increments for measurements at 50 keV, in 4 volt increments at 100 keV and in 6 volt increments at 150 keV. Ten volt increments were used at 75 and 125 keV because the distribution of energy losses was not expected to vary enough as a function of energy to justify detailed measurements at all five energies.

The analyzers were cross calibrated to the high voltage supply of an accelerator operated by the ORNL Thermonuclear Division. This supply was regulated to one part in one hundred thousand and had a voltage divider that had been calibrated using p, gamma resonance reactions. The transmission of protons with energies from 50 to 200 keV was measured as a function of the voltage applied to the analyzer electrodes. The energy calibration of the accelerator voltage divider was checked by measuring the gamma rays produced by resonance proton interactions with thick targets of fluorine and aluminum. Measured resonance energies were in close agreement with the published values thus corroborating the original calibration.

At energies above 1 MeV and in cases where mean energy loss rather than an energy-loss distribution is desired, protons can enter and exit the gas cell via thin foils. The energy lost by the protons in these foils can be determined, but the resulting fluctuations in the energy loss would have to be extracted from those produced in the gas. At the energies for which this experiment was designed, the energy-loss fluctuations produced in the foils could completely mask the effects of the gas. Moreover, the foils would have to be extremely thin and thus undependable. To avoid these problems, the proton beam was allowed to enter and leave the gas cell via holes 0.71 mm in diameter. The gas cell had differential pumping sections on its input and output to handle the gas escaping through the holes. The temperature, T, of the gas in the cell could be measured to 0.1°K, but could not be controlled; pressure, P, could be measured in increments of 10^{-4} Torr and regulated to $\pm 5 \times 10^{-4}$ Torr.

The system was aligned to a 50 keV proton beam from the accelerator by making adjustments to center the beam on a plastic scintillator as each section was assembled. Data were taken by measuring the transmitted current with a Faraday cup coupled to a vibrating reed electrometer with digitized output. A series of tests showed that the best signal available for normalizing the measurements to variations in accelerator output was the current that wiped off on a special electrode mounted between the input aperture and the electrodes of the output analyzer. This current reflected both current and energy fluctuations in the beam. Normalization currents were also measured using a vibrating reed electrometer with digitized output.

The analyzers were cross calibrated to the high voltage supply of an accelerator operated by the ORNL Thermonuclear Division. This supply was regulated to one part in one hundred thousand and had a voltage divider that had been calibrated using p, gamma resonance reactions. The transmission of protons with energies from 50 to 200 keV was measured as a function of the voltage applied to the analyzer electrodes. The energy calibration of the accelerator voltage divider was checked by measuring the gamma rays produced by resonance proton interactions with thick targets of fluorine and aluminum. Measured resonance energies were in close agreement with the published values thus corroborating the original calibration.

At energies above 1 MeV and in cases where mean energy loss rather than an energy-loss distribution is desired, protons can enter and exit the gas cell via thin foils. The energy lost by the protons in these foils can be determined, but the resulting fluctuations in the energy loss would have to be extracted from those produced in the gas. At the energies for which this experiment was designed, the energy-loss fluctuations produced in the foils could completely mask the effects of the gas. Moreover, the foils would have to be extremely thin and thus undependable. To avoid these problems, the proton beam was allowed to enter and leave the gas cell via holes 0.71 mm in diameter. The gas cell had differential pumping sections on its input and output to handle the gas escaping through the holes. The temperature, T, of the gas in the cell could be measured to 0.1°K , but could not be controlled; pressure, P, could be measured in increments of 10^{-4} Torr and regulated to $\pm 5 \times 10^{-4}$ Torr.

The system was aligned to a 50 keV proton beam from the accelerator by making adjustments to center the beam on a plastic scintillator as each section was assembled. Data were taken by measuring the transmitted current with a Faraday cup coupled to a vibrating reed electrometer with digitized output. A series of tests showed that the best signal available for normalizing the measurements to variations in accelerator output was the current that wiped off on a special electrode mounted between the input aperture and the electrodes of the output analyzer. This current reflected both current and energy fluctuations in the beam. Normalization currents were also measured using a vibrating reed electrometer with digitized output.

The gases measured, their purities, and the suppliers are given in Table 1. Most of the gases were greater than 99% pure, although two of some interest, propyne and propadiene, were not. No attempt was made to make corrections for the impurities in these gases.

Lodhi and Powers⁹ used propadiene of similar purity in their measurements of alpha stopping cross sections and found that the impurities affected the cross sections by just over 1%.

TABLE 1. Gases, Purities and Suppliers

Gas	Purity	Matheson
Hydrogen (H_2)	99.999%	Matheson
Methane (CH_4)	99.97%	Matheson
Ethyne ($HC:CH$)	99.6%	Matheson
Ethene ($CH_2:CH_2$)	99.98%	Matheson
Ethane (CH_3CH_3)	99.96%	Matheson
Propyne ($CH_3C:CH$)	96%	Air Products and Chemicals
Propadiene ($CH_2:C:CH_2$)	97%	Linde
Propene ($CH_3CH:CH_2$)	99.9%	Lif-O- Gen
Cyclopropane (CH_2) ₃	99.9%	Matheson
Propane ($CH_3CH_2CH_3$)	99.99%	Matheson

Data was taken with the gas density in the cell adjusted to give a 4% energy loss at each proton energy. To determine the required gas densities required good values of the stopping powers. Such data were not always available in the literature, so a preliminary measurement was made for each gas.

Once the proper gas densities were obtained, acquisition of data for the energy-loss distributions began. Data were taken with three consecutive measurements at each voltage, beginning and ending with electrometer zero-offset measurements. Each series of readings from 50 to 150 keV was repeated three times. These data were treated as nine individual sets by a program that calculated the distributions, normalized them to a unit sum and then calculated the mean energy and second and third central moments for each. These data were accumulated and the means and standard deviations calculated. The error calculations included reasonable estimates of the uncertainties in the energy values and excluded any of the data that fell outside limits described by Chauvenet's criteria.²¹

Results and Conclusions

To convert energy loss to stopping cross sections requires a division by the density of the gas and the length of the gas cell. The physical length of the gas cell was 31.39 ± 0.03 cm. However, an estimate of the effect of the gas streaming through the aperture was made by assuming that the decrease in the pressure as

Propyne ($\text{CH}_3\text{C}:\text{CH}$)	96%	Air Products and Chemicals
Propadiene ($\text{CH}_2:\text{C}:\text{CH}_2$)	97%	Linde
Propene ($\text{CH}_3\text{CH}:\text{CH}_2$)	99.9%	Lif-O- Gen
Cyclopropane (CH_2) ₃	99.9%	Matheson
Propane ($\text{CH}_3\text{CH}_2\text{CH}_3$)	99.99%	Matheson

Data was taken with the gas density in the cell adjusted to give a 4% energy loss at each proton energy. To determine the required gas densities required good values of the stopping powers. Such data were not always available in the literature, so a preliminary measurement was made for each gas.

Once the proper gas densities were obtained, acquisition of data for the energy-loss distributions began. Data were taken with three consecutive measurements at each voltage, beginning and ending with electronmeter zero-offset measurements. Each series of readings from 50 to 150 keV was repeated three times. These data were treated as nine individual sets by a program that calculated the distributions, normalized them to a unit sum and then calculated the mean energy and second and third central moments for each. These data were accumulated and the means and standard deviations calculated. The error calculations included reasonable estimates of the uncertainties in the energy values and excluded any of the data that fell outside limits described by Chauvenet's criteria.²¹

Results and Conclusions

To convert energy loss to stopping cross sections requires a division by the density of the gas and the length of the gas cell. The physical length of the gas cell was 31.39 ± 0.03 cm. However, an estimate of the effect of the gas streaming through the aperture was made by assuming that the decrease in the pressure as a function of distance from, X , from the aperture could be described by

$$P(x) = P_0 \left(\frac{x}{0.036} \right)^n .$$

The gas cell pressure was P_0 and the value 0.036 represented the radius of the aperture.

2

The fittings required for aligning the apparatus to the beam produced an asymmetry in the distances from the gas cell apertures

to the ion gauges in their respective differential pumping sections. As a result, the value of n could be computed for one side and used to calculate a pressure for the other side as a test of the hypothesis. This was done for a number of gas cell pressures and gases and in every case the values obtained for n were near -1.4.

Making these corrections resulted in an increase in the cell length of 0.16 cm. While this increase is only 0.5%, it was added to the measured length of the cell with the assumption that each component of the increase was known with the same uncertainty as the measurement.

Another problem is to determine at what energy the measured stopping-power value applies. A common method is to assign the value to the average energy $(E_0 + \langle E \rangle)/2$. This is valid if the stopping power changes only a small amount over the energy region from E_0 to $\langle E \rangle$. Since relatively small energy

losses were involved in this experiment and only small variations in stopping power were involved over the entire range of the experiment, this simple technique is undoubtedly adequate. To accommodate this approach and to allow data to be presented at even energy values, the data were taken at proton energies of 51, 76.5, 102, 127.5 and 153 keV.

As mentioned by Bichsel,²² when the proton energy is below 0.5 MeV, charge exchange might play a significant role in energy loss. Weyl²³ discusses this and estimates a contribution of about

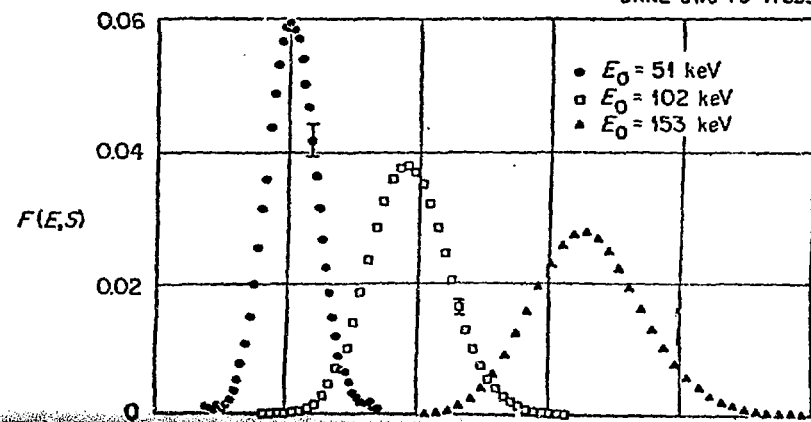
8%. A recent paper by Vollmer²⁴ gives an estimate of the effect of charge exchange on energy-loss fluctuations of 100 keV protons in hydrogen.

Nuclear collisions can also play an important part in the energy loss of very slowly moving particles.²⁵

However, these effects will be minimal in an experiment such as this that has a relatively thick absorber and measures only highly-collimated, forward-going protons.

Some typical energy-loss distributions (for ethane) are shown in Figure 2. The distributions

ORNL-DWG 75-17635



component of the increase was known with the same uncertainty as the measurement.

Another problem is to determine at what energy the measured stopping-power value applies. A common method is to assign the value to the average energy $(E_0 + \langle E \rangle)/2$. This is valid if the stopping power changes only a small amount over the energy region from E_0 to $\langle E \rangle$. Since relatively small energy

losses were involved in this experiment and only small variations in stopping power were involved over the entire range of the experiment, this simple technique is undoubtedly adequate. To accommodate this approach and to allow data to be presented at even energy values, the data were taken at proton energies of 51, 76.5, 102, 127.5 and 153 keV.

As mentioned by Bichsel,²² when the proton energy is below 0.5 MeV, charge exchange might play a significant role in energy loss. Weyl²³ discusses this and estimates a contribution of about 8%. A recent paper by Vollmer²⁴ gives an estimate of the effect of charge exchange on energy-loss fluctuations of 100 keV protons in hydrogen. Nuclear collisions can also play an important part in the energy loss of very slowly moving particles.²⁵ However, these effects will be minimal in an experiment such as this that has a relatively thick absorber and measures only highly-collimated, forward-going protons.

Some typical energy-loss distributions (for ethane) are shown in Figure 2. The distributions

2

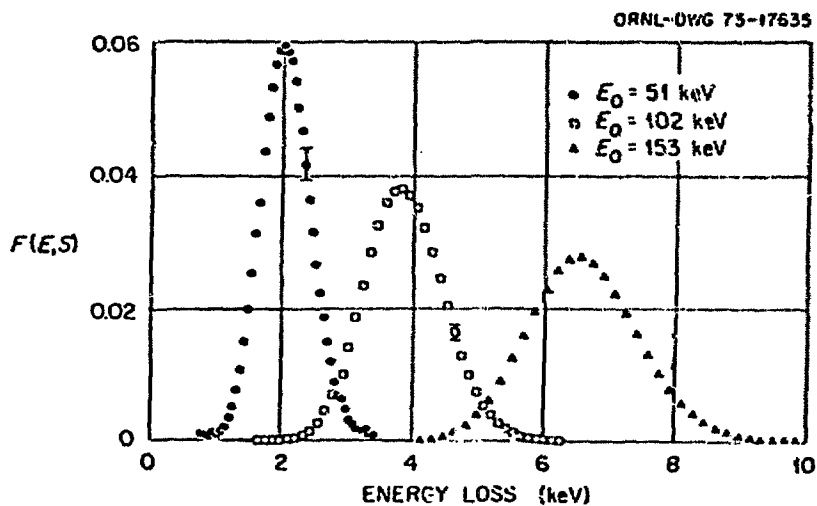


Fig. 2 Energy-Loss Distributions, $F(E,S)$, for Protons in Ethane as a Function of $E-⟨E⟩$.

have unit area and the uncertainties shown are one standard deviation and represent the worst case. Second and third central moments of the stopping distributions were calculated from the data obtained at input proton energies of 51, 102 and 153 keV. The data for ethyne, ethene and ethane are tabulated in Table 2.

TABLE 2. Experimental and Theoretical Second and Third Central Moments
(keV² and keV³, Respectively)

Proton	E(keV) 50	100	150
Ethyne			
A_2 Ex	0.136 \pm 0.010	0.331 \pm 0.033	0.620 \pm 0.071
A_2 Th	0.116	0.319	0.604
$-A_3$ Ex	0.011 \pm 0.007	0.040 \pm 0.034	0.114 \pm 0.114
$-A_3$ Th	0.009	0.037	0.102
Ethene			
A_2 Ex	0.136 \pm 0.010	0.345 \pm 0.033	0.609 \pm 0.070
A_2 Th	0.119	0.296	0.547
$-A_3$ Ex	0.011 \pm 0.007	0.044 \pm 0.035	0.109 \pm 0.100
$-A_3$ Th	0.008	0.034	0.092
Ethane			
A_2 Ex	0.154 \pm 0.010	0.360 \pm 0.034	0.701 \pm 0.072
A_2 Th	0.113	0.277	0.573
$-A_3$ Ex	0.014 \pm 0.008	0.046 \pm 0.037	0.137 \pm 0.111
$-A_3$ Th	0.007	0.031	0.096

Large uncertainties occur in these values because the uncertainties in the energy values compound rapidly when the energy is squared or cubed.²⁶ Except for ethyne, the A_2 values exceed the theoretical values by 10 to 40%. The A_3 values range from 10% to 250% times the theory.

Aside from questions about the applicability of the theory in this case, some of the differences observed might be due to nuclear scattering and molecular binding effects. Charge exchange by the proton might increase the width of the distributions, and thus A_2 , but it should decrease the skew (A_3) because protons that had traveled a portion of the gas cell without charge would have lost less energy and would appear on the high energy side of the distribution. Negative A_3 values indicate asymmetry towards the low energy side of the distribution.

Proton	E(keV)	50	100	150
Ethyne				
A_2	Ex	0.136 \pm 0.010	0.331 \pm 0.033	0.620 \pm 0.071
A_2	Th	0.136	0.319	0.604
$-A_3$	Ex	0.011 \pm 0.007	0.040 \pm 0.034	0.114 \pm 0.114
$-A_3$	Th	0.009	0.037	0.102
Ethene				
A_2	Ex	0.136 \pm 0.010	0.345 \pm 0.033	0.609 \pm 0.070
A_2	Th	0.119	0.296	0.547
$-A_3$	Ex	0.011 \pm 0.007	0.044 \pm 0.035	0.109 \pm 0.100
$-A_3$	Th	0.008	0.034	0.092
Ethane				
A_2	Ex	0.154 \pm 0.010	0.360 \pm 0.034	0.701 \pm 0.072
A_2	Th	0.113	0.277	0.573
$-A_3$	Ex	0.014 \pm 0.008	0.046 \pm 0.037	0.137 \pm 0.111
$-A_3$	Th	0.007	0.031	0.096

Large uncertainties occur in these values because the uncertainties in the energy values compound rapidly when the energy is squared or cubed.²⁶ Except for ethyne, the A_2 values exceed the theoretical values by 10 to 40%. The A_2 values range from 10% to 250% times the theory.

Aside from questions about the applicability of the theory in this case, some of the differences observed might be due to nuclear scattering and molecular binding effects. Charge exchange by the proton might increase the width of the distributions, and thus A_2 , but it should decrease the skew (A_3) because protons that had traveled a portion of the gas cell without charge would have lost less energy and would appear on the high energy side of the distribution. Negative A_3 values indicate asymmetry towards the low energy side of the distribution.

In the simplest approximation, the value of M_2 is a constant and the value of $A_2(S)$ is just $2M_2S$. Therefore, these data can be tested by dividing by S and seeing if the results are reasonably constant. In all cases, the values of A_2/S obtained at 100 and 150 keV were the same for any gas. Similarly, a simple form for $A_3(S)$ is proportional to ES . When the measured values were divided by this factor, a constant value was found for each gas. This conclusion has to be somewhat dependent by the large uncertainties;

2

involved.

Stopping cross sections calculated from the energy loss data by using the relation

$$\epsilon = (3.282 \pm 0.005) \times 10^{-18} (E_0 - \langle E \rangle) T/P$$

are shown in Table 3. The errors represent one standard deviation and are not percent standard error as is often quoted for this type of data.

TABLE 3. Measured Stopping Cross Sections in Units of
 $10^{-15} \text{ eV-cm}^2 \text{ Molecule}^{-1}$

E_p	Hydrogen	Methane	Ethyne	Ethene
50	14.1 \pm 0.4	37.4 \pm 1.0	46.2 \pm 0.9	54.1 \pm 1.1
75	12.4 \pm 0.5	36.3 \pm 0.9	45.6 \pm 1.5	54.3 \pm 2.0
100	10.8 \pm 0.2	35.9 \pm 0.9	42.7 \pm 0.8	51.4 \pm 1.0
125	9.7 \pm 0.3	34.1 \pm 0.5	40.2 \pm 1.3	48.5 \pm 1.3
150	8.6 \pm 0.1	32.0 \pm 0.4	37.4 \pm 0.7	44.9 \pm 0.9

E_p	Ethane	Propyne	Propadiene	Propene
50	61.6 \pm 1.3	69.7 \pm 2.4	67.3 \pm 1.7	76.8 \pm 2.7
75	63.0 \pm 2.0	69.8 \pm 2.3	65.8 \pm 2.3	74.0 \pm 4.9
100	59.7 \pm 1.2	65.6 \pm 1.5	64.5 \pm 1.2	75.0 \pm 1.6
125	56.3 \pm 1.4	61.7 \pm 1.7	63.2 \pm 2.8	70.9 \pm 1.9
150	52.6 \pm 0.9	57.4 \pm 1.1	59.3 \pm 2.1	66.6 \pm 1.4

E_p	Cyclopropane	Propane
50	71.1 \pm 2.4	84.5 \pm 2.2
75	70.1 \pm 3.5	86.4 \pm 3.5
100	69.0 \pm 2.4	83.0 \pm 2.3
125	65.7 \pm 2.6	78.8 \pm 2.6
150	62.7 \pm 1.4	72.9 \pm 1.8

The uncertainties include those calculated for the energy loss, a 0.2°C uncertainty in temperature measurements, a 0.1% manometer error and the 5×10^{-14} Torr uncertainty in how closely the gas cell pressure could be registered.

Given $\epsilon(H)$, $\epsilon(C)$ can be found from the equation.

$$\epsilon(C) = \frac{\epsilon(C_m H_n) - n\epsilon(H)}{m}$$

Values obtained from such a calculation are shown in Table 4.

shown in Table 3. The errors represent one standard deviation and are not percent standard error as is often quoted for this type of data.

TABLE 3. Measured Stopping Cross Sections in Units of
 $10^{-15} \text{ eV-cm}^2 \text{ Molecule}^{-1}$

E_p	Hydrogen	Methane	Ethyne	Ethene
50	14.1 \pm 0.4	37.4 \pm 1.0	46.2 \pm 0.9	54.1 \pm 1.1
75	12.4 \pm 0.5	36.3 \pm 0.9	45.6 \pm 1.5	54.3 \pm 2.0
100	10.8 \pm 0.2	35.9 \pm 0.9	42.7 \pm 0.8	51.4 \pm 1.0
125	9.7 \pm 0.3	34.1 \pm 0.5	40.2 \pm 1.3	48.5 \pm 1.3
150	8.6 \pm 0.1	32.0 \pm 0.4	37.4 \pm 0.7	44.9 \pm 0.9
E_p	Ethane	Propyne	Propadiene	Propene
50	61.6 \pm 1.3	69.7 \pm 2.4	67.3 \pm 1.7	76.8 \pm 2.7
75	63.0 \pm 2.0	69.8 \pm 2.3	65.8 \pm 2.3	74.0 \pm 4.9
100	55.7 \pm 1.2	65.6 \pm 1.5	64.5 \pm 1.2	75.0 \pm 1.6
125	56.3 \pm 1.4	61.7 \pm 1.7	63.2 \pm 2.8	70.9 \pm 1.9
150	52.6 \pm 0.9	57.4 \pm 1.1	59.3 \pm 2.1	66.6 \pm 1.4
E_p	Cyclopropane	Propane		
50	71.1 \pm 2.4	84.5 \pm 2.2		
75	70.1 \pm 3.5	86.4 \pm 3.5		
100	69.0 \pm 2.4	83.0 \pm 2.3		
125	65.7 \pm 2.6	78.8 \pm 2.6		
150	62.7 \pm 1.4	72.9 \pm 1.8		

The uncertainties include those calculated for the energy loss, a 0.2°C uncertainty in temperature measurements, a 0.1% manometer error and the 5×10^{-14} Torr uncertainty in how closely the gas cell pressure could be registered.

Given $\epsilon(H)$, $\epsilon(C)$ can be found from the equation.

$$\epsilon(C) = \frac{\epsilon(C_{m,n}) - n\epsilon(H)}{m}$$

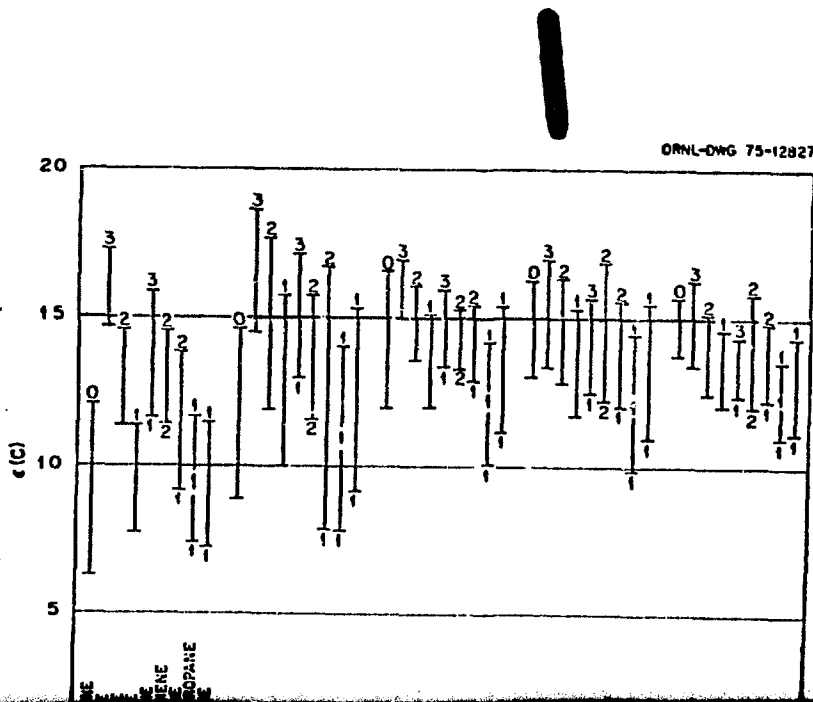
Values obtained from such a calculation are shown in Table 4.

2

TABLE 4. Carbon Stopping Cross Sections Calculated Assuming Bragg Additivity

E_p	Methane- $2H_2$	$1/2$ (Ethyne- H_2)	$1/2$ (Ethane- $2H_2$)
50	9.2 ± 1.1	15.0 ± 0.5	13.0 ± 0.6
75	11.8 ± 1.1	16.6 ± 0.8	14.8 ± 1.1
100	14.3 ± 0.9	16.0 ± 0.4	14.9 ± 0.5
125	14.7 ± 0.6	15.2 ± 0.7	14.6 ± 0.7
150	14.8 ± 0.4	14.4 ± 0.4	13.8 ± 0.5
E_p	$1/2$ (Ethane- $3H_2$)	$1/3$ (Propyne- $2H_2$)	$1/3$ (Propadiene- $2H_2$)
50	9.6 ± 0.7	13.8 ± 0.8	13.0 ± 0.6
75	12.9 ± 1.1	15.0 ± 0.8	13.7 ± 0.8
100	13.6 ± 0.6	14.7 ± 0.5	14.3 ± 0.4
125	13.6 ± 0.7	14.1 ± 0.6	14.6 ± 0.9
150	13.4 ± 0.5	13.4 ± 0.4	14.0 ± 0.7
E_p	$1/3$ (Propene- $3H_2$)	$1/3$ (Cyclopropane- $3H_2$)	
50	11.5 ± 0.9	9.6 ± 0.8	
75	12.3 ± 1.7	11.0 ± 1.2	
100	14.2 ± 0.5	12.2 ± 0.8	
125	13.9 ± 0.7	12.2 ± 0.9	
150	13.6 ± 0.5	12.3 ± 0.5	
E_p	$1/3$ (Propane- $4H_2$)		
50	9.4 ± 0.8		
75	12.3 ± 1.2		
100	13.3 ± 0.8		
125	13.3 ± 0.9		
150	12.8 ± 0.6		

Differences in the values calculated for $\epsilon(C)$ can be correlated with the type of carbon bonds involved in the molecule. This is shown clearly in Figure 3



75	12.9 \pm 1.1	15.0 \pm 0.8	13.7 \pm 0.8
100	13.6 \pm 0.6	14.7 \pm 0.5	14.3 \pm 0.4
125	13.6 \pm 0.7	14.1 \pm 0.6	14.6 \pm 0.9
150	13.4 \pm 0.5	13.4 \pm 0.4	14.0 \pm 0.7

wh:
wh:
th:

E_p 1/3(Propene-3H₂) 1/3(Cyclopropane-3H₂)

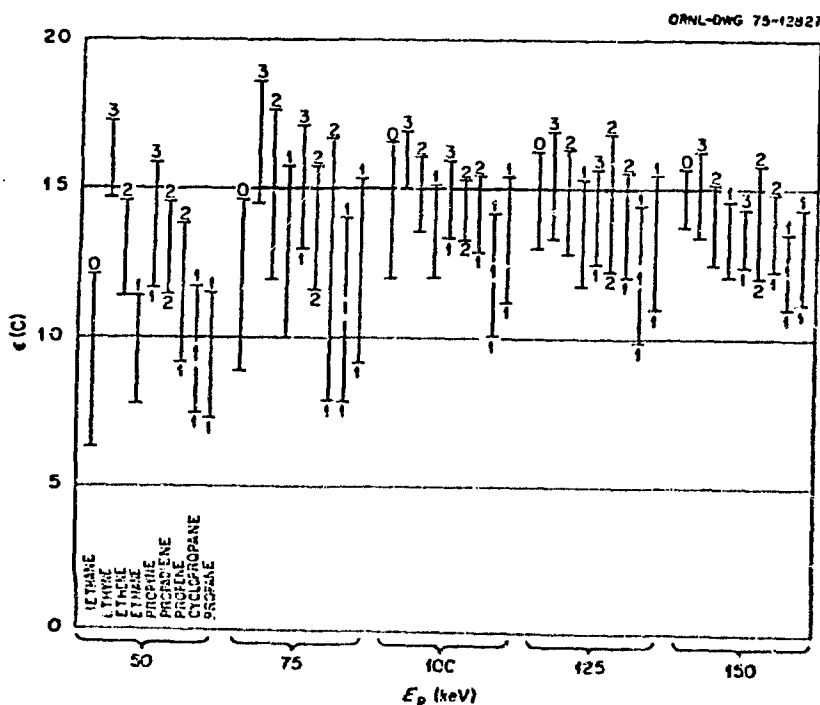
of
pos
rat
cyc
sta
The
wei
bor
wei
Fig
tak
bor

50	11.5 \pm 0.9	9.6 \pm 0.8
75	12.3 \pm 1.7	11.0 \pm 1.2
100	14.2 \pm 0.5	12.2 \pm 0.8
125	13.9 \pm 0.7	12.2 \pm 0.9
150	13.6 \pm 0.5	12.3 \pm 0.5

E_p 1/3(Propane-4H₂)

50	9.4 \pm 0.8
75	12.3 \pm 1.2
100	13.3 \pm 0.8
125	13.3 \pm 0.9
150	12.8 \pm 0.6

Differences in the values calculated for $\epsilon(C)$ can be correlated with the type of carbon bonds involved in the molecule. This is shown clearly in Figure 3



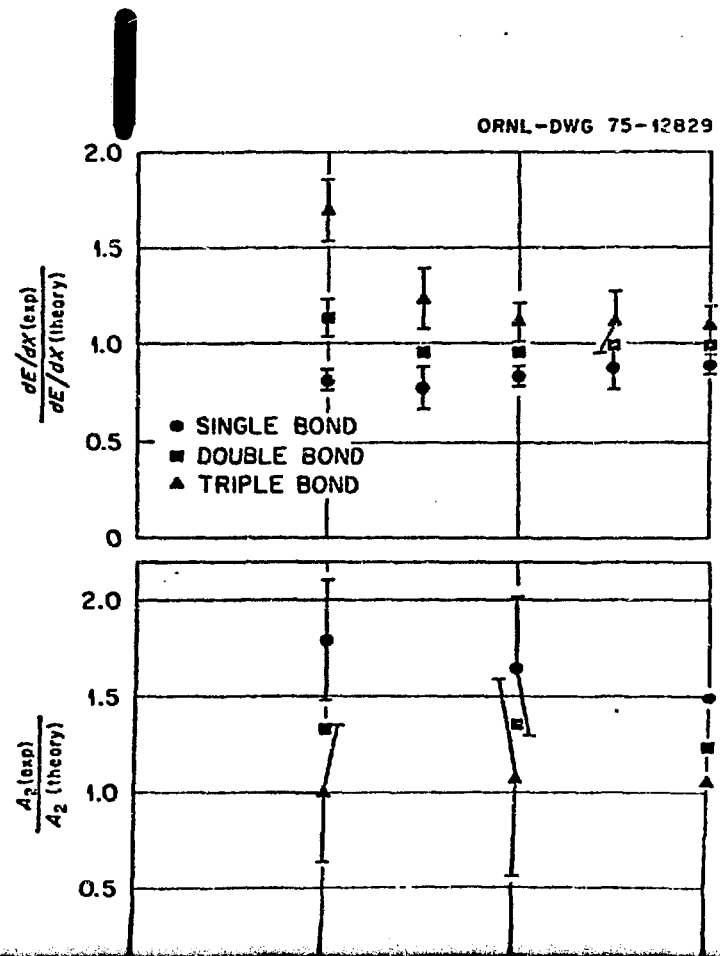
2

Fig. 3. Diagram of $\epsilon(C)$ Values Obtained from the Data. The Length of the Lines Represents the 90% Confidence Interval, i.e., the range in which the true value is expected to lie.

Fig.

which is a diagram of the $\epsilon(C)$ data. The length of the lines represents a 99% confidence interval and the numbers represent the type of carbon bonds involved. A statistically significant difference between the stopping cross sections for triple, double and single carbon bonds is shown at 50 keV. The uncertainties do not permit a definite statement to be made at higher energies, but the trends remain the same. The diagram also shows that propadiene, with two double bonds, gives $\epsilon(C)$ values like those from ethene rather than like its isomer, propyne. Moreover, the value obtained from propyne, which has a single and a triple bond, falls between the values of ethyne, which has a triple bond, and ethane or propane, which have only single bonds. Similar trends are noted when the data of Park and Zimmerman⁷ are treated in this manner.

Another interesting comparison was the ratios of measured to calculated values for the stopping power and second and third central moments. For the ratios of stopping power it was found that ethane, cyclopropane and propane gave the same ratio, within statistical limits, always less than 1 for any energy. The ratios for ethene and propadiene also agreed but were significantly larger than those for the single bonded molecules and nearer to one. Values from ethyne were considerably larger than one. This is shown in Figure 4. Relatively small uncertainties result from taking weighted averages of the data for each type of bonding.



when the data of Park and Zimmerman⁷ are treated in this manner.

Another interesting comparison was the ratios of measured to calculated values for the stopping power and second and third central moments. For the ratios of stopping power it was found that ethane, cyclopropane and propane gave the same ratio, within statistical limits, always less than 1 for any energy. The ratios for ethene and propadiene also agreed but were significantly larger than those for the single bonded molecules and nearer to one. Values from ethyne were considerably larger than one. This is shown in Figure 4. Relatively small uncertainties result from taking weighted averages of the data for each type of bonding.

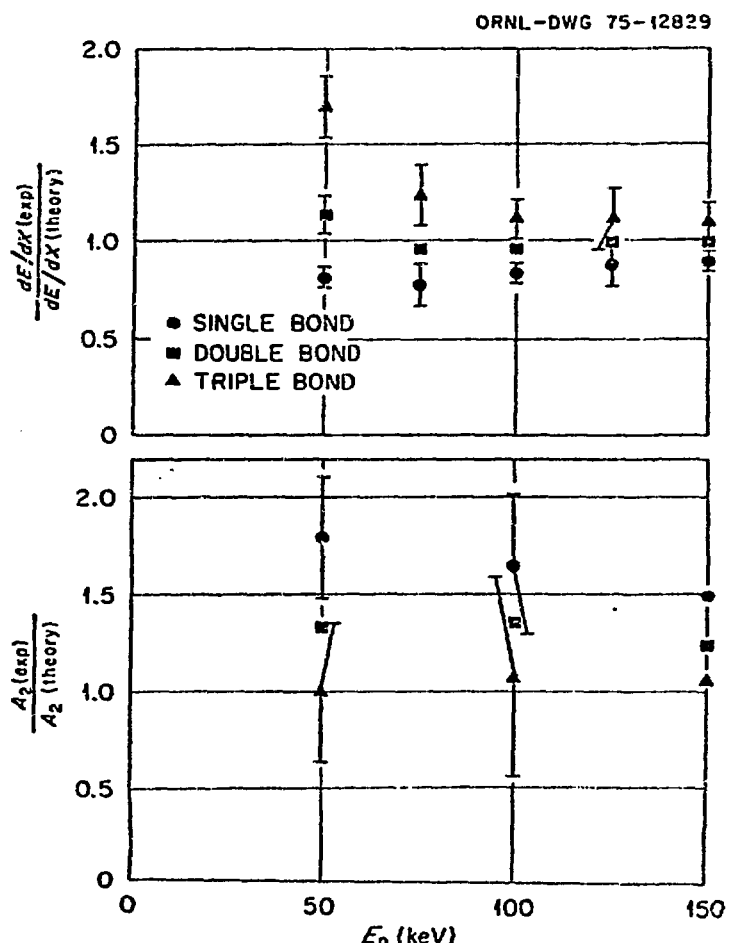


Fig. 4. Ratios of dE/dx (Exp) to dE/dx (Theory) and A_2 (Exp) to A_2 (Theory) as a Function of Proton Energy.

Ratios of measured to theoretical second central moments are also shown in Figure 4. In this case, the single bonded molecules gave ratios as much as 1.4 while the ethyne ratios were all near one. The double bonded molecules fell in between as usual. As before, the uncertainties shown on the graph represent the 99% confidence interval. Ratios of measured to calculated values of the third central moment showed the same trends, but the uncertainties were too large to allow any definite conclusions. In every case, the ratios for methane were most like the double bonded values, propyne fell midway between the single and triple bonded values and propene fell midway between the single and double bonded values.

The most obvious conclusion reached from the measurements of the energy-loss distributions was that the theory did not match the data. Large uncertainties must always be involved in the determination of the higher moments of the experimental distribution which may make comparisons with theory difficult or meaningless. However, the internal consistency of the data was good even when compared with the simplest possible theory. It has been suggested that the length of the gas cell coupled with the small aperture size could result in the rejection of a significant number of the protons that had undergone "hard" collisions so that these measurements are predominated by protons that had undergone only soft collisions. Some treatments of these data are now underway that show this might have indeed been a problem, primarily with the collisions involving the sigma electrons in the carbon-carbon bonds. However, some other experiments, such as Park and Schowengerd⁴, have similar acceptance angles. This experiment was the first of its type and deficiencies of this nature should be investigated in later work.

Some of the most interesting results of this experiment were those related to the additivity of stopping cross sections. Statistically significant differences for compounds with different types of carbon bonding were found at 50 keV. Although the uncertainties in the data prevent positive conclusions at the other energies, the trends of the data are consistent with an effect due to bonding at all of the energies measured. Variations with bond types were found in the stopping-cross-section data, regardless of whether the standard of comparison was experimental or theoretical. Correlated variations also occurred in the comparisons of the second and third central moments of the distribution with theory. Details of this work are given in ORNL/TM-5165.²⁷

Because of the assumed additivity of stopping powers is a useful tool for dosimetry, more stopping cross section measurements should be made to include

bonded values, propene fell midway between the single and triple bonded values and propene fell midway between the single and double bonded values.

The most obvious conclusion reached from the measurements of the energy-loss distributions was that the theory did not match the data. Large uncertainties must always be involved in the determination of the higher moments of the experimental distribution which may make comparisons with theory difficult or meaningless. However, the internal consistency of the data was good even when compared with the simplest possible theory. It has been suggested that the length of the gas cell coupled with the small aperture size could result in the rejection of a significant number of the protons that had undergone "hard" collisions so that these measurements are predominated by protons that had undergone only soft collisions. Some treatments of these data are now underway that show this might have indeed been a problem, primarily with the collisions involving the sigma electrons in the carbon-carbon bonds. However, some other experiments, such as Park and Schowengerd⁴, have similar acceptance angles. This experiment was the first of its type and deficiencies of this nature should be investigated in later work.

Some of the most interesting results of this experiment were those related to the additivity of stopping cross sections. Statistically significant differences for compounds with different types of carbon bonding were found at 50 keV. Although the uncertainties in the data prevent positive conclusions at the other energies, the trends of the data are consistent with an effect due to bonding at all of the energies measured. Variations with bond types were found in the stopping-cross-section data, regardless of whether the standard of comparison was experimental or theoretical. Correlated variations also occurred in the comparisons of the second and third central moments of the distribution with theory. Details of this work are given in ORNL/TM-5165.²⁷

2

Because of the assumed additivity of stopping powers is a useful tool for dosimetry, more stopping cross section measurements should be made to include all of the elements of tissue. Other gases that should be run are oxygen and nitrogen, the oxides of nitrogen and carbon, ammonia, cyanogen and possibly water vapor. More data on hydrocarbon gases and vapors would also be useful. There are several gases available that have more carbon bonds per molecule, such as butadiene and butane, and many heavier hydrocarbons have sufficient vapor pressure to allow measurements. The alpha measurements of

Lodhi and Powers⁹ do include butadiene and butane. Heavier hydrocarbons would also include cyclic molecules in addition the linear molecules that comprised the greatest part of this work.

Questions left unanswered by the size of the uncertainties in the present data might be resolved by repeating some of the measurements. The maximum information on additivity would probably be obtained by limiting the gases to hydrogen, ethyne, ethene, ethane, propadiene, cyclopropane and propane and limiting the proton energies to the range between 40 and 100 keV.

Like most experiments, this one answered several questions, but, in the process, raised others. Despite the many years of effort that have gone into stopping-power measurements, it is still a fertile field for useful, meaningful and interesting research.

References

1. Bohr, N., Phil. Mag. 25, 10 (1913).
2. Bragg, W. H. and R. Kleeman, Phil. Mag. 10, 318 (1905).
3. Geiger, H. M., Proc. Roy. Soc. A83, 505 (1910).
4. Park, J. T. and F. D. Schowengerdt, Rev. Sci. Inst. 40, 753 (1969).
5. Crenshaw, C. M., Phys. Rev. 62, 54 (1942).
6. Reynolds, H. K., D. N. F. Dunbar, W. A. Wenzel and W. Whaling, Phys. Rev. 92, 742 (1953).
7. Park, J. T. and E. J. Zimmerman, Phys. Rev. 131, 1611 (1963).
8. Bourland, P. D. And D. Powers, Phys. Rev. B3, 3635 (1971).
9. Lodhi, A. S. and D. Powers, Phys. Rev. A10, 2131 (1974).
10. Bethe, H. A., Ann. der Phys. 5, 325 (1930).
11. Turner, J. E., P. D. Roecklein, and R. B. Vora, Health Phys. 18, 159 (1970).
12. Turner, J. E., Health Phys. 13, 1255 (1967).
13. Landau, L., J. Phys. USSR 8, 201 (1944).
14. Vavilov, P. V., Soviet Phys. JETP 5, 749 (1957).
15. Bohr, N., Phil. Mag. 30, 581 (1915).
16. Tschalär, C., Nucl. Instr. and Meth. 61, 141 (1968).
17. Payne, M. G., Phys. Rev. 185, 611 (1969).
18. Symon, K. R., Ph.D. Thesis, Harvard 1948 (unpublished).
19. Summarized in: B. Rossi, "High-Energy Particles" (pg. 29) Prentice Hall, New York (1952).
20. Seigbahn, K., "Alpha, Beta, Gamma Ray Spectroscopy", (Ed. K. Seigbahn), p. 172, North-Holland, Amsterdam (1966).
21. Worthing, J. A., and J. Geffner, "Treatment of Experimental Data", John Wiley and Sons, New York (1943).
22. Bichsel, H., "Studies in Penetration of Charged Particles in Matter". (Ed. U. Fano) NAS-NRC-1133, pg. 17 (1964).
23. Weyl, P. K., Phys. Rev. 91, 289 (1953).
24. Vollmer, O., Nucl. Instr. and Meth. 121, 373 (1974).
25. Bohr, N., Mat. Fys. Medd. Dan. Vid. Selsk. 18, No. 8 (1948).

3. Geiger, H. M., Proc. Roy. Soc. A83, 505 (1910).
4. Park, J. T. and F. D. Schowengerdt, Rev. Sci. Inst. 40, 753 (1969).
5. Crenshaw, C. M., Phys. Rev. 62, 54 (1942).
6. Reynolds, H. K., D. N. F. Dunbar, W. A. Wenzel and W. Whaling, Phys. Rev. 92, 742 (1953).
7. Park, J. T. and E. J. Zimmerman, Phys. Rev. 131, 1611 (1963).
8. Bourland, P. D. And D. Powers, Phys. Rev. B3, 3635 (1971).
9. Lodhi, A. S. and D. Powers, Phys. Rev. A10, 2151 (1974).
10. Bethe, H. A., Ann. der Phys. 5, 325 (1930).
11. Turner, J. E., P. D. Roecklein, and R. S. Vora, Health Phys. 18, 159 (1970).
12. Turner, J. E., Health Phys. 13, 1255 (1967).
13. Landau, L., J. Phys. USSR 8, 201 (1944).
14. Vavilov, P. V., Soviet Phys. JETP 5, 749 (1957).
15. Bohr, N., Phil. Mag. 30, 581 (1915).
16. Tschalär, C., Nucl. Instr. and Meth. 61, 141 (1968).
17. Payne, M. G., Phys. Rev. 185, 611 (1969).
18. Symon, K. R., Ph.D. Thesis, Harvard 1948 (unpublished).
19. Summarized in: B. Rossi, "High-Energy Particles" (pg. 29) Prentice Hall, New York (1952).
20. Seigbahn, K., "Alpha, Beta, Gamma Ray Spectroscopy", (Ed. K. Seigbahn), p. 172, North-Holland, Amsterdam (1966).
21. Worthing, J. A., and J. Geffner, "Treatment of Experimental Data", John Wiley and Sons, New York (1943).
22. Bichsel, H., "Studies in Penetration of Charged Particles in Matter". (Ed. U. Fano) NAS-NRC-1133, pg. 17 (1964).
23. Weyl, P. K., Phys. Rev. 91, 289 (1953).
24. Vollmer, O., Nucl. Instr. and Meth. 121, 373 (1974).
25. Bohr, N., Mat. Fys. Medd. Dan. Vid. Selsk. 18, No. 8 (1948).
26. Beers, Y., "Introduction to the Theory of Error", Addison-Wesley, Reading, Mass. (1957).
27. Thorngate, J. H., "Measurement of Energy Losses, Distributions of Energy Loss and Additivity of Energy Losses for 50 to 150 keV protons in Hydrogen and Nine Hydrocarbon Gases", ORNL/TM-5165 (May 1976).